

Computational and Experimental Characterization of a Fluorescent Dye for Detection of Potassium Ion Concentration

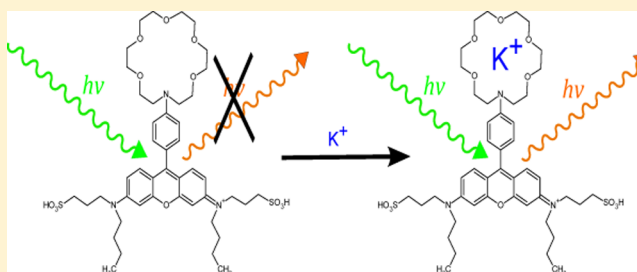
Matteus Tanha,[†] Subhasish K. Chakraborty,[‡] Beth Gabris,[§] Alan S. Waggoner,[‡] Guy Salama,[§] and David Yaron^{*,†}

[†]Chemistry Department and [‡]Molecular Biosensor and Imaging Center, Carnegie Mellon University, Pittsburgh, Pennsylvania 15213, United States

[§]Department of Cell Biology and Physiology, School of Medicine, University of Pittsburgh, Pittsburgh, Pennsylvania 15260, United States

S Supporting Information

ABSTRACT: The fluorescence of the SKC-513 ((*E*)-*N*-(9-(4-(1,4,7,10,13-pentaoxa-16-azacyclooctadecan-16-yl)phenyl)-6-(butyl(3-sulfopropyl)amino)-3*H*-xanthen-3-ylidene)-*N*-(3-sulfopropyl)butan-1-ammonium) dye is shown experimentally to have high sensitivity to binding of the K⁺ ion. Computations are used to explore the potential origins of this sensitivity and to make some suggestions regarding structural improvements. In the absence of K⁺, excitation is to two nearly degenerate states, a neutral (N) excited state with a high oscillator strength, and a charge-transfer (CT) state with a lower oscillator strength. Binding of K⁺ destabilizes the CT state, raising its energy far above the N state. The increase in fluorescence quantum yield upon binding of K⁺ is attributed to the increased energy of the CT state suppressing a nonradiative pathway mediated by the CT state. The near degeneracy of the N and CT excited states can be understood by considering SKC-513 as a reduced symmetry version of a parent molecule with 3-fold symmetry. Computations show that acceptor–donor substituents can be used to alter the relative energies of the N and CT state, whereas a methylene spacer between the heterocycle and phenylene groups can be used to increase the coupling between these states. These modifications provide synthetic handles with which to optimize the dye for K⁺ detection.



OVERVIEW

Fluorescence imaging provides a set of powerful techniques for monitoring biological processes in living organisms.^{1–6} These techniques rely on dye molecules that change their fluorescence behavior under varying environments. For neural processes, it is useful to have dyes whose fluorescence tracks the concentration of the K⁺ ion. The experimental data presented below for the dye SKC-513 (Figure 1) show a substantial change in quantum yield as the K⁺ concentration varies between 0 and 1000 mM. The dye has a crown ether portion that binds the potassium ion and a chromophore that signals the presence of the ion. We use quantum chemical calculations to explore the mechanism through which the ion alters the fluorescence of the chromophore.

The computations presented below indicate that SKC-513 is a photoinduced electron-transfer (PET) sensor, a class of dyes whose fluorescence quantum yield is known to be sensitive to ion binding.^{4–6} In these dyes, the change in quantum yield arises from the competition between a radiative pathway, emission from a neutral excited state (N) created on photoexcitation, and a nonradiative pathway, which is mediated by a charge-transfer (CT) excited state. Ion binding destabilizes the CT state and alters the branching ratio between the radiative and nonradiative pathways. The computations

presented here find that the lowest-energy excitations of SKC-513 correspond to a fluorescent state with predominantly N character and a less optically intense state with predominantly CT character. The potassium ion preferentially destabilizes the CT state, thereby altering the quantum yield, consistent with the mechanism implicated in other PET sensors.

A feature of the excited states of SKC-513 that may be contributing to the high sensitivity of the fluorescence quantum yield to ion binding is a near degeneracy of the N state, which mediates the radiative pathway, and the CT state, which mediates a nonradiative pathway. The binding of K⁺ substantially raises the energy of the CT state, suppressing the nonradiative pathway. The near degeneracy of the N and CT states may appear to be accidental, given that SKC-513 has only a 2-fold symmetry axis. However, comparison to a 3-fold symmetric parent reveals a systematic origin. In the parent molecule, the lowest excited state is doubly degenerate. In addition, the molecular orbitals involved in these degenerate excitations have low density in the regions of the molecule that

Received: July 27, 2014

Revised: September 8, 2014

Published: September 12, 2014

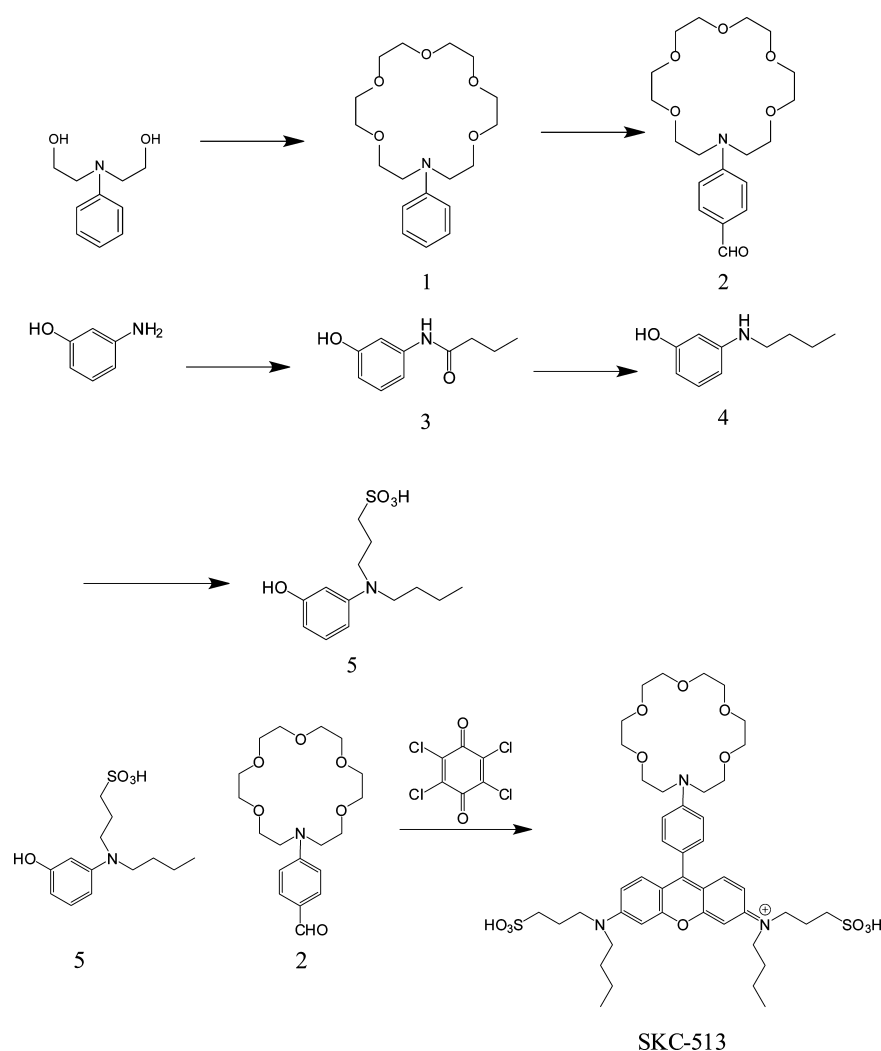


Figure 1. Primary steps in the synthesis of SKC-513.

must be altered to convert the parent molecule to SKC-513. The degeneracy of excited states in SKC-513 is therefore not accidental but can be traced back to degeneracies expected for this 3-fold symmetric parent.

Our calculations also find that replacing the potassium ion with a point charge has little effect on the nature of the relevant excited states. This suggests that changes in the excited states of the chromophore in SKC-513 arise from field effects of the potassium ion, as opposed to more specific interactions such as ligation with the nitrogen atom that connects the crown ether to the chromophore.

■ SYNTHESIS OF SKC-513

Figure 1 illustrates the primary steps in the synthesis of SKC-513 described in this section.

Synthesis of Compound 1: 16-Phenyl-1,4,7,10,13-pentaoxa-16-azacyclooctadecane. In a 2 L three-neck round-bottom flask fitted with a reflux condenser, 8 g of NaH (60% in mineral oil, 2 mmol) was added to 400 mL of anhydrous THF and the mixture was refluxed under argon. *N*-Phenyldiethanolamine (18.17 g, 1 mmol) and 50.631 g of tetra(ethylene glycol)-di-*p*-tosylate (1 mmol) dissolved in 400 mL of anhydrous THF were added to the refluxed NaH solution over a period of 8 h, and the resulting mixture was refluxed for another 24 h. After the reaction mass was cooled

and filtered, the solid was washed with 100 mL of THF. The combined organic filtrate was concentrated and the oily residue was subjected to silica gel column chromatography using diethyl ether as eluent, providing a light yellow oil (10.361 g, 31% yield) as compound 1. ^1H NMR δ (CDCl_3): 3.702 (m, 24H), 6.697 (m, 2H), 7.22 (m, 1H), 7.37 (m, 1H), 7.805 (d, 1H). EI MS: m/z 339.73 (M^+).

Synthesis of Compound 2: 4-(1,4,7,10,13-Pentaoxa-16-azacyclooctadecan-16-yl)benzaldehyde. Compound 1 (3.414 g) (1 mmol) was dissolved in 45 mL of DMF, and the solution was cooled to -5°C using a salt ice bath under stirring. POCl_3 (18.93 g) was added to the reaction solution over a period of 1 h while the reaction temperature was maintained between -5 and 0°C . The solution was removed from the ice bath, stirred at room temperature for 20 h, warmed to 70°C , and stirred for an additional 2 h. The solution was then cooled and added to 450 g of ice water, basified with Na_2CO_3 to pH 7.5, and extracted with 3×300 mL of CHCl_3 . The combined organic layer was then washed with 3×200 mL water, dried over anhydrous MgSO_4 , and concentrated to provide 5.31 g of crude product. This was purified by silica gel column chromatography using CH_2Cl_2 to give 3.687 g of product (100% yield) as a light yellow oil. ^1H NMR, δ (CDCl_3): 3.67 (m, 24H), 6.743 (d, 2H), 7.73 (d, 2H), 9.73 (s, 1H, CHO). EI MS: m/z 367.92 (M^+).

Synthesis of Compound 3: *N*-(3-Hydroxyphenyl)-butyramide. *n*-Butyric anhydride (20.23 g) was added dropwise to a solution of 3-aminophenol (10.93 g) in 400 mL of dry THF at 0 °C over a period of 1 h. After stirring at room temperature for 20 h, the solution was concentrated under reduced pressure. The residue was resuspended in 300 mL of CHCl_3 , and the suspension was stirred at room temperature for 2 h, at which point the white solid that formed was filtered and dried to provide 14.13 g of colorless crystals as compound 3. MW $\text{C}_{10}\text{H}_{13}\text{NO}_2$: 179.0946 g/mol. ^1H NMR, δ ($\text{DMSO}-d_6$): 0.912 (t, 3H), 1.60 (q, 2H), 2.257 (t, 2H), 6.41 (m, 1H), 6.930 (m, 1H), 7.04 (m, 1H), 7.19 (m, 1H), 9.303 (s, 1H), 9.696 (s, 1H). ESI-MS: m/z 179.34 (M^+).

Synthesis of Compound 4: 3-(Butylamino)phenol. NaBH_4 (5.03 g) and compound 3 [*N*-(3-hydroxyphenyl)butyramide] (10.31 g) were taken in 100 mL of dry THF, and the mixture was cooled to 0 °C. I_2 (10.57 g) in 80 mL of dry THF was added at 0 °C for 1 h under argon. The mixture was refluxed for 3 h and cooled to room temperature. HCl (3 M, 30 mL) was added carefully over a period of 30 min. The mixture was neutralized by 1 M NaOH and extracted with 2×250 mL of ethyl acetate. The combined organic extract was washed with brine and water, dried over anhydrous MgSO_4 , and concentrated to dryness, providing a crude colorless oil that was purified by silica gel column chromatography using *n*-hexane/ether (3:1 v/v) to give 7.33 g of product (compound 4) as a colorless solid. MW $\text{C}_{10}\text{H}_{15}\text{NO}$: 165.1154 g/mol. ^1H NMR, δ (CDCl_3): 1.007 (t, 3H), 1.46 (m, 2H), 1.62 (m, 2H), 3.11 (t, 2H), 6.16 (m, 1H), 6.22 (m, 2H), 7.037 (t, 1H). ESI-MS: m/z 165.54 (M^+).

Synthesis of Compound 5: 3-(Butyl(3-hydroxyphenyl)amino)propane-1-sulfonic acid. Compound 4 (3.32 g) and 1,3-propanesultone (2.88 g) were dissolved in 15 mL of dry DMF, and the solution was heated at 130 °C for 20 h, then cooled to room temperature, and concentrated. The resulting crude residue was purified by a PR C-18 column using 50% water in methanol as solvent, to give 3.23 g of a light brown oily residue that solidified upon standing (compound 5). MW $\text{C}_{13}\text{H}_{21}\text{NO}_4\text{S}$: 287.1191 g/mol. ^1H NMR, δ ($\text{DMSO}-d_6$): 0.83 (m, 3H), 1.25 (m, 4H), 1.75 (m, 4H), 3.41–3.64 (m, 4H), 6.89 (d, 1H), 7.06 (m, 2H), 7.41 (m, 1H). ESI-MS: m/z 287.33 (M^+).

Synthesis of SKC-513. Compound 2 (370 mg), compound 5 (704 mg), and PTSA (100 mg) were dissolved in 25 mL of propionic acid, and the solution was stirred at 70 °C for 20 h. After concentrating, 150 mL of 3 M NaOAc aqueous solution was added to the residue and the mixture was stirred for 1 h at room temperature. After the solution was concentrated, the residue was subjected to silica gel column chromatography using $\text{CH}_2\text{Cl}_2/\text{MeOH}$ (3:1 v/v), providing a purple gummy residue that was used immediately for subsequent reaction with tetrachloro-1,4-benzoquinone (530 mg) in a methanol/chloroform (1:1) mixture at ambient temperature for 15 h. Excess tetrachloro-1,4-benzoquinone was removed by filtration, and the reaction mixture was concentrated under reduced pressure. The residue was purified twice by Silica gel column chromatography using 30% MeOH in CHCl_3 as solvent to get a crimson to dark violet solid as product SKC-513 (113 mg). ^1H NMR, δ (CD_3OD): 0.93 (t, 6H), 1.38 (m, 4H), 1.72 (m, 4H), 2.02 (t, 4H), 2.93 (m, 4H), 3.54–3.82 (m, 32H), 7.03 (m, 4H), 7.17 (d, 2H), 7.40 (d, 2H), 7.67 (d, 2H). ESI-MS: m/z 902.51 ($\text{M} - 2\text{H}$).

EXPERIMENTAL CHARACTERIZATION

The fluorescence intensity of SKC-513 as a function of ion concentration is shown in Figures 2 and 3. Figure 2 highlights

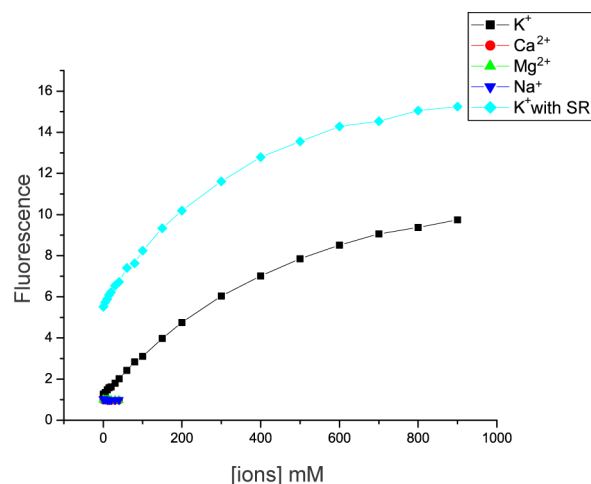


Figure 2. Experimental data for SKC-513 showing the fluorescence intensity (in arbitrary units) as a function of the concentration of various ions in the range from 0 to 1000 mM. SR refers to experiments done in the presence of a sarcoplasmic reticulum.

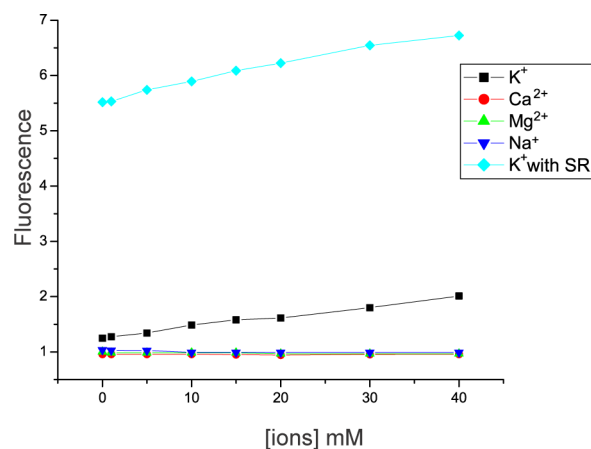


Figure 3. As in Figure 2, but over an ion concentration range 0–40 mM.

how fluorescence intensity increases with K^+ concentration, saturating at about 1000 mM, giving an enhancement of nearly an order of magnitude in the fluorescence intensity. Figure 3 shows that the binding is selective over the biologically relevant range of concentrations, with no change in fluorescence intensity found for Ca^{2+} , Mg^{2+} , or Na^+ . Also shown is the effects of K^+ on fluorescence intensity in the presence of the sarcoplasmic reticulum (SR), isolated via the procedure described in Salama et al.⁷ The experiment was conducted in a solution composed of the isolated SR with 5 μM ion (KCl , NaCl , CaCl_2 , or MgCl_2) in 100 mM dye, 20 mM HEPES, and 1 mM gluconic acid.

COMPUTATIONAL METHODS

Unless otherwise indicated, all calculations used density functional theory (DFT) for the ground electronic state and time dependent DFT (TDDFT) for excited states, with the CAM-B3LYP functional⁸ and a 6-31G** basis. CAM-B3LYP

has previously been shown to provide good results for excitation energies of conjugated dyes.⁹ For all calculations reported below, the polarizable continuum model (PCM),¹⁰ as implemented in Gaussian 09,¹¹ was used with water as solvent.

The structure of the SKC-513 dye is shown in Figure 1. The ion binds to the crown ether at the top of the dye. To facilitate the calculations, the structure was simplified to contain only the optical chromophore shown in Figure 4, which will be referred

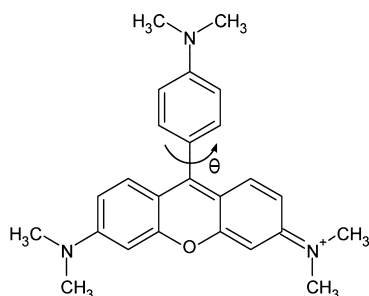


Figure 4. Structure of the simplified SKC-513 dye (SSKC-513).

to as simplified-SKC-513 (SSKC-513). Effects of ion binding were modeled either by explicit inclusion of a potassium ion or by including the electrical potential arising for a point charge placed at a location corresponding to the center of the crown ether. The charge was positioned at a distance of 3 Å from the nitrogen of the crown ether, along an axis connecting the nitrogen to the oxygen of the heterocycle. The distance of 3 Å was taken from experimental and theoretical studies on potassium crown ether complexes.^{12–14}

Torsion about the angle θ of Figure 4 is relatively facile with a minimum at 52° and the range 30° to 80° being populated at room temperature. Because the energy and oscillator strengths of the lowest-energy excited states are only weakly dependent on θ (Supporting Information), the results shown below are for either the geometry-optimized ground or excited state.

The Supporting Information also includes results from semiempirical calculations that were used in initial exploration of the photophysics. The semiempirical and DFT results lead to similar conclusions regarding the way in which binding of potassium ion alters the fluorescence properties. This agreement across quite different quantum chemical models indicates that the conclusions are robust with respect to the level of theory employed.

COMPUTATIONAL RESULTS

Effects of a Point Charge. Figure 5 shows the effect of a point charge placed at a position corresponding to the center of the crown ether in SKC-513. In the absence of a point charge, there are two nearly degenerate excited states. These states have different oscillator strengths and relative positions that are strongly dependent on the sign and magnitude of the charge. Following Kasha's rule,¹⁵ we expect the molecule to fluoresce strongly only when the lowest excited electronic state carries significant optical intensity. This rule assumes that excitation to the optically intense excited state is followed by relaxation to the lowest excited electronic state on a time scale that is much faster than the fluorescence lifetime. If the lowest excited state has a strong optical transition to the ground state, fluorescence will occur. As the optical intensity of the lowest excited state decreases, more population is lost to nonradiative pathways and the fluorescence quantum yield decreases.

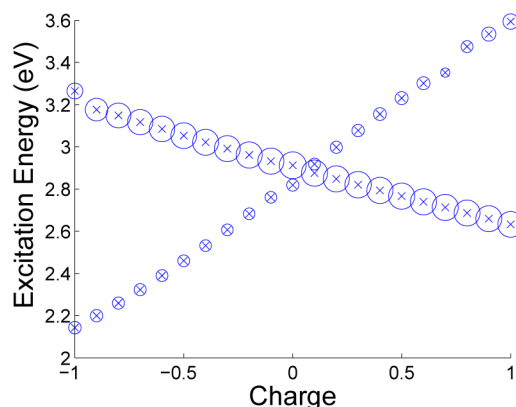


Figure 5. Effects of a point charge on the excited states of SSKC-513. (The radii of the circles are proportional to the oscillator strength.)

In the absence of a point charge, the lowest-energy state is the less intense state, which implies the molecule should be only weakly fluorescent. As the magnitude of the point charge is increased in the positive direction, the bright state drops below the less intense state, suggesting that the presence of a cation such as potassium should substantially enhance the fluorescence quantum yield. We next explore the origin of the excited-state degeneracy and then consider calculations that use an explicit K^+ ion instead of a point charge.

Origin of the Degenerate Excited States. Examination of the frontier orbitals allows assignment of neutral (N) and charge-transfer (CT) character to the excited states of Figure 5. These states are essentially pure excitations between the orbitals shown in Figure 6. For vertical excitation in the absence

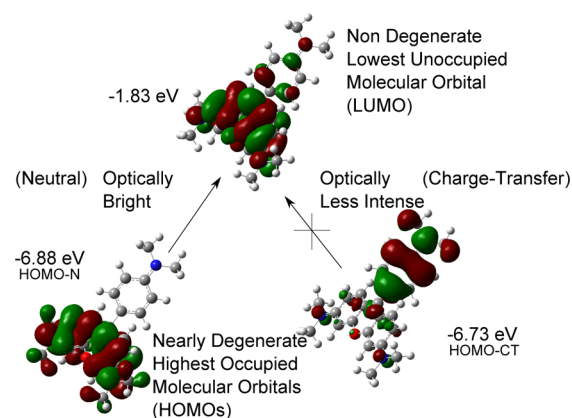


Figure 6. Frontier orbitals of SSKC-513. There are two nearly degenerate HOMOs, one located on the heterocycle and the other on the phenylene ring. The LUMO is nondegenerate and located on the heterocycle. Optical intensity relies on good overlap between orbitals, such that only the transition from HOMO-N to the LUMO carries large optical intensity.

of a point charge, the first excited state has 95% HOMO-CT \rightarrow LUMO character and the second excited state has 97% HOMO-N \rightarrow LUMO character. The lowest unoccupied molecular orbital (LUMO) resides on the heterocycle. HOMO-CT resides primarily on the phenylene ring, such that the HOMO-CT \rightarrow LUMO corresponds to transfer of charge from the phenyl ring to the heterocycle, indicating a CT state. Because there is little overlap between HOMO-CT and the LUMO, this CT state carries little optical intensity.

HOMO-N resides on the heterocycle, such that HOMO-N \rightarrow LUMO corresponds to a neutral (N) excitation, with substantially more oscillator strength than the CT state.

The effects of the point charge in Figure 5 can also be understood in terms of the frontier orbitals. Because a positive charge bound to the crown ether is closer to the phenylene ring than to the heterocycle, it preferentially lowers the energy of the HOMO-CT. This raises the energy of the HOMO-CT \rightarrow LUMO transition that dominates the CT state. This is in agreement with Figure 5, which shows that a positive charge causes the less intense CT state to rise significantly above the bright N state.

The near degeneracy of the two lowest-excited states observed in SSKC-513 may be unexpected, because the excitations have a largely different character, one being a N excitation on the heterocycle and the other being a CT excitation from the heterocycle to the phenylene ring. Furthermore, SSKC-513 has at most 2-fold symmetry, and degeneracies are not expected for C_2 symmetry groups. However, doubly degenerate states are expected for molecules with 3-fold symmetry, because the C_3 symmetry groups have doubly degenerate representations. The molecule of Figure 7

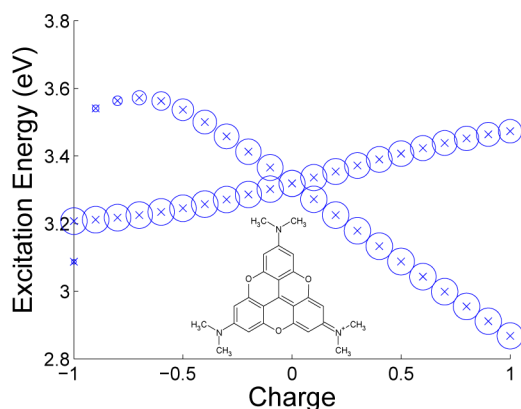


Figure 7. Effects of a point charge on the excited states of the 3-fold symmetric parent of SSKC-513. (The radii of the circles are proportional to oscillator strength.)

uses bridging oxygen atoms to convert SSKC-513 to a 3-fold symmetric system. The orbitals of this symmetric parent molecule are shown in Figure 8. The HOMO is again doubly degenerate, whereas the LUMO is nondegenerate. The nodal pattern of the HOMOs also reveals why removal of oxygen and

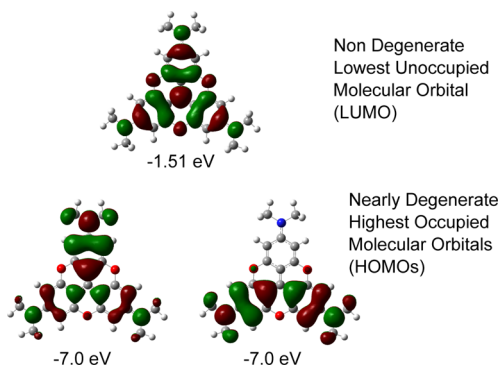


Figure 8. Frontier molecular orbitals of the 3-fold symmetric parent of SSKC-513.

rotation of the upper phenylene ring to form SSKC-513 does not substantially lift the degeneracy: the HOMOs have little amplitude in the regions of the additional oxygen atoms. The nearly degenerate HOMOs of SSKC-513 are therefore not an accidental degeneracy, but rather a result of the 3-fold symmetry of this parent molecule.

The effects of a point charge on the 3-fold symmetric parent molecule are shown in Figure 7. The point charge lifts the degeneracy, similar to the behavior of SSKC-513 in Figure 5. However, both states retain optical intensity such that binding of the ion would not be expected to have a strong effect on the fluorescent behavior. The 3-fold symmetric molecule is therefore useful for understanding the origin of the degenerate excited states of SSKC-513, but is not expected to be a useful chromophore for ion detection.

Effects of a Potassium Ion. Above, the effects of ion binding were explored by examining the effects of a point charge located at a position corresponding to the center of the crown ether. The results suggest that a positive charge preferentially stabilizes HOMO-CT, which resides primarily on the phenylene ring (Figure 6). This causes the less intense CT state to rise above the bright N state (Figure 5), which rationalizes the observed increase in fluorescence quantum yield upon binding of a cation.

Results from DFT calculations that explicitly include a K^+ ion (Figure 9) lead to similar conclusions. Figure 9 shows the lowest two excited states, S_1 and S_2 , with CT and N character assigned on the basis of the predicted optical intensity and examination of the orbitals that contribute to the excitation (Supporting Information). Results are shown for both the ground- electronic-state geometry, corresponding to vertical excitation, and the relaxed S_1 geometry, corresponding to fluorescence.

In the presence of K^+ (right side of Figure 9), the gap between S_1 and S_2 is large, with S_1 having strong N character and so carrying substantial oscillator strength. We therefore expect high fluorescence quantum yield in the presence of a K^+ ion, for reasons that are consistent with those obtained above based on the effects of a point charge.

In the absence of K^+ (left side of Figure 9), the gap between S_1 and S_2 is small, being 0.05 eV for the ground-state geometry and 0.15 eV for the relaxed S_1 geometry. In the ground-state geometry, the S_1 and S_2 states have the same character as seen in the presence of a point charge: S_1 has CT character and carries 2.5 times less intensity than the S_2 state, which has N character. Upon excited-state relaxation, the S_1 and S_2 states are predicted to cross: S_1 has N character and carries 2.5 times more intensity than the S_2 state, which now has CT character. The weaker fluorescence seen in the absence of a K^+ ion can then be attributed to the near degeneracy of S_1 and S_2 , with the energy separation being so close that they cross as the geometry relaxes from that of the vertical excitation to that of the S_1 state.

Because torsions associated with θ of Figure 4 are low-frequency, it is plausible that the excited-state relaxation is dominated by motion along this coordinate. However, the change in torsional angles are relatively small. In the absence of a K^+ ion, the relaxation of the torsional angle is from 54° to 57.5° and in the presence of a K^+ ion, the relaxation is from 63° to 60.7° .

Also of interest is the degree to which the interaction with K^+ goes beyond field effects to include more specific chemical interactions. The molecular orbitals that participate in the excitation have negligible amplitude on the potassium ion

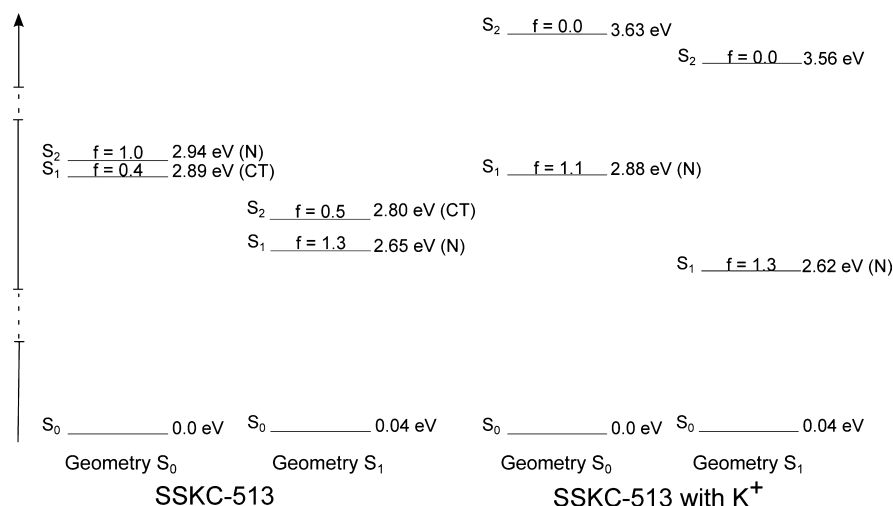


Figure 9. Electronic states of SSKC-513 (Figure 5) with (right) and without (left) a K^+ ion at a location corresponding to the center of the crown ether in SKC-513.

(Supporting Information). This, along with the similar behavior observed for a point charge, suggests that the effects of the ion on the excited state arise primarily from the electric field of the ion.

Effects of Electronic Substituents. The suggested mechanism for the effects of K^+ on the fluorescence quantum yield is that the electric field of the ion causes the molecule to move from the less-emissive regime on the left of Figure 5 to the more emissive regime on the right. The computations reported here are approximate, not only in the methods used for the electronic structure of the chromophore but also for the use of a continuum dielectric model for the solvent and the use of a simplified structure for the dye (Figure 4). Although such approximations likely do not invalidate the proposed mechanism, they do suggest that the predicted location of the crossing point between the less emissive and more emissive regimes may not be highly reliable. A reasonable target for synthetic modification to SKC-513 is adding substituents that alter the crossing point. This can be done by adding electronic acceptors or donors that alter the relative energies of the HOMOs in Figure 6.

Two derivatives of SSKC-513 are compared with SSKC-513 in Figure 10. The results can be understood in terms of the effects of the substituents on the HOMOs of Figure 6. Addition of fluorine atoms to the phenylene group stabilizes the HOMO-CT located on the phenylene ring (the HOMO on the right in Figure 6), thereby raising the energy of the CT state relative to that of the N state. Similarly, addition of fluorine atoms to the heterocycle stabilizes the HOMO-N shown on the left of Figure 6, thereby raising the N state relative to the CT state.

These results suggest that electronic substituents provide a handle that may be used to optimize the sensitivity of SSKC-513 fluorescence to ion binding, by altering the relative energies of the N and CT states.

Effects of a Bridging Methylene. Figure 11 shows the effects of a point charge on the excited states when an extra methylene group is placed between the heterocycle and the phenylene group. The calculations are done for the optimized geometry, in which the phenylene ring is nearly perpendicular to the heterocycle. The avoided crossing between N and CT states suggests a stronger electronic coupling between these

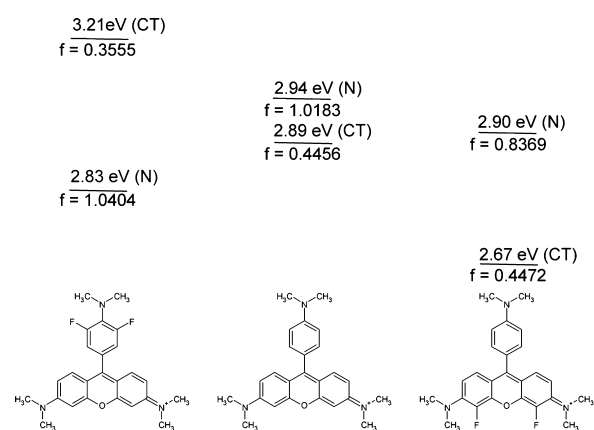


Figure 10. Effects of Fluorine substituents on the two lowest excited states of SSKC-513. Adding F substituents to the phenylene ring (left) raises the energy of the CT excited state, and adding F substituents to the heterocycle has the opposite effect.

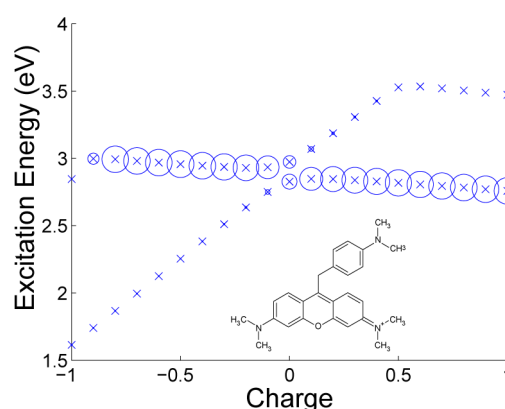


Figure 11. Two lowest excited states of a modified SSKC-513, in which a methylene bridges between the phenylene group and the heterocycle. (The radii of the circles are proportional to the oscillator strength.)

states than is seen in Figure 5 for SSKC-513. A more detailed examination of the curve crossings suggests a coupling of 0.15 eV for this system, compared to about 0.01 eV for SSKC-513. The proposed mechanism for ion sensitivity assumes rapid

relaxation between N and CT states. A stronger coupling between N and CT states may enhance this relaxation, such that the addition of a bridge methylene group may enhance the sensitivity of fluorescence to ion binding.¹⁶ The introduction of a bridging methylene also leads to a substantial decrease in the oscillator strength of the CT state. This increased contrast between the N and CT states may also enhance the sensitivity of fluorescence to ion binding.

CONCLUSIONS

The quantum chemical calculations presented here suggest a mechanism for the sensitivity of SKC-513 to ion binding, and a possible means for enhancing this sensitivity. The mechanism relates to the near degeneracy of a bright excitation, corresponding to a N excitation on the heterocycle of SKC-513, and a CT excitation corresponding to charge transfer from the phenylene group to the heterocycle. In the absence of K⁺, these two states lie close in energy. Binding of K⁺ destabilizes the CT excited state, raising its energy far above the N state. In the presence of K⁺, the lowest-energy excited state has high oscillator strength and is well separated from other electronic states. This rationalizes the increase in fluorescence intensity seen experimentally upon binding of K⁺. Computations suggest that electronic substituents may be used to alter the relative location of the N and CT states, whereas the introduction of a methylene group as a bridge between the heterocycle and the phenylene group alters the electronic coupling between these states. Such modifications may therefore provide synthetic handles with which to optimize the sensitivity of the fluorescence to ion binding.

ASSOCIATED CONTENT

Supporting Information

Computed torsional potential for SSKC-513, two lowest excited-state energies of SSKC-513 as a function of torsional angle, semiempirical calculations of SSKC-513 in the presence of a point charge, and comparison of molecular orbitals and electronic excitations of SSKC-513 in the absence and presence of K⁺. This material is available free of charge via the Internet at <http://pubs.acs.org>

AUTHOR INFORMATION

Corresponding Author

*D. Yaron. E-mail: aron@cmu.edu.

Notes

The authors declare no competing financial interest.

ACKNOWLEDGMENTS

This work was supported by the National Institutes of Health (Grant No. 1R01HL093074-01) and the National Science Foundation (Grant No. 1027985).

REFERENCES

- (1) Ntziachristos, V. Fluorescence Molecular Imaging. *Annu. Rev. Biomed. Eng.* **2006**, *8*, 1–33.
- (2) Wache, N.; Scholten, A.; Klüner, T.; Koch, K.-W.; Christoffers, J. Turning On Fluorescence with Thiols - Synthetic and Computational Studies on Diaminoterephthalates and Monitoring the Switch of the Ca²⁺ Sensor Recoverin. *Eur. J. Org. Chem.* **2012**, *2012*, 5712–5722.
- (3) Olsen, S.; Smith, S. C. Radiationless Decay of Red Fluorescent Protein Chromophore Models via Twisted Intramolecular Charge-Transfer States. *J. Am. Chem. Soc.* **2007**, *129*, 2054–65.

- (4) de Silva, A. P.; Gunnlaugsson, T.; Rice, T. E. Recent Evolution of Luminescent Photoinduced Electron Transfer Sensors. A Review. *Analyst* **1996**, *121*, 1759.
- (5) de Silva, A. P.; Moody, T. S.; Wright, G. D. Fluorescent PET (Photoinduced Electron Transfer) Sensors as Potent Analytical Tools. *Analyst* **2009**, *134*, 2385–93.
- (6) Bissell, R.; Prasanna de Silva, A.; Nimal Gunaratne, H.; Mark Lynch, P.; Maguire, G.; McCoy, C.; Samankumara Sandanayake, K. Fluorescent PET (Photoinduced Electron Transfer) Sensors. *Curr. Top. Med. Chem.* **1993**, *168*, 223–264.
- (7) Salama, G.; Scarpa, A. Enhanced Ca²⁺ Uptake and ATPase Activity of Sarcoplasmic Reticulum in the Presence of Diethyl Ether. *J. Biol. Chem.* **1980**, *255*, 6525–6528.
- (8) Yanai, T.; Tew, D. P.; Handy, N. C. A New Hybrid Exchange-Correlation Functional Using the Coulomb-Attenuating Method (CAM-B3LYP). *Chem. Phys. Lett.* **2004**, *393*, 51–57.
- (9) Jacquemin, D.; Perpète, E. A.; Scuseria, G. E.; Ciofini, I.; Adamo, C. TD-DFT Performance for the Visible Absorption Spectra of Organic Dyes: Conventional versus Long-Range Hybrids. *J. Chem. Theory Comput.* **2008**, *4*, 123–135.
- (10) Tomasi, J.; Mennucci, B.; Cancès, E. The IEF Version of the PCM Solvation Method: an Overview of a New Method Addressed to Study Molecular Solutes at the QM Ab Initio Level. *J. Mol. Struct.* **1999**, *464*, 211–226.
- (11) Frisch, M. J.; et al.; *Gaussian 09*, Revision A.1; Gaussian Inc.: Wallingford, CT, 2009.
- (12) Glendening, E. D.; Feller, D.; Thompson, M. A. An Ab Initio Investigation of the Structure and Alkali Metal Cation Selectivity of 18-Crown-6. *J. Am. Chem. Soc.* **1994**, *116*, 10657–10669.
- (13) Thompson, M. A.; Glendening, E. D.; Feller, D. The Nature of K⁺ Crown Ether Interactions: A Hybrid Quantum Mechanical-Molecular Mechanical Study. *J. Phys. Chem.* **1994**, *98*, 10465–10476.
- (14) Steed, J. W. First- and Second-Sphere Coordination Chemistry of Alkali Metal Crown Ether Complexes. *Coord. Chem. Rev.* **2001**, *215*, 171–221.
- (15) Kasha, M. Characterization of Electronic Transitions in Complex Molecules. *Discuss. Faraday Soc.* **1950**, *9*, 14–19.
- (16) Marcus, R. A. Electron Transfer Reactions in Chemistry. Theory and Experiment. *Rev. Mod. Phys.* **1993**, *65*, 599–610.